Article

Screening of Type I and II Drug Binding to Human Cytochrome P450-3A4 in Nanodiscs by Localized Surface Plasmon Resonance Spectroscopy

Aditi Das, Jing Zhao, George C. Schatz, Stephen G. Sligar, and Richard P. Van Duyne

Anal. Chem., **2009**, 81 (10), 3754-3759• DOI: 10.1021/ac802612z • Publication Date (Web): 13 April 2009

Anal. Chem. **2009,** *81,* 3754–3759

Screening of Type I and II Drug Binding to Human Cytochrome P450-3A4 in Nanodiscs by Localized Surface Plasmon Resonance Spectroscopy

Aditi Das,[†] Jing Zhao,[‡,§] George C. Schatz,[*,§] Stephen G. Sligar,[*,†] and Richard P. Van Duyne[*,§]

Department of Biochemistry and Chemistry, Beckman Institute for Advanced Science and Technology, University of Illinois Urbana−Champaign, Urbana, Illinois 61801, and Department of Chemistry, Northwestern University, 2145 Sheridan Road, Evanston, Illinois 60208-3113

A prototype nanoparticle biosensor based on localized surface plasmon resonance (LSPR) spectroscopy was developed to detect drug binding to human membrane-bound cytochrome P450 3A4 (CYP3A4). CYP3A4 is one of the most important enzymes in drug and xenobiotic metabolism in the human body. Because of the inherent propensity of CYP3A4 to aggregate, it is difficult to study drug binding to this protein in solution and on surfaces. In this paper, we use a soluble nanometer scale membrane bilayer disk (Nanodisk) to functionally stabilize monomeric CYP3A4 on Ag nanoparticle surfaces fabricated by nanosphere lithography. CYP3A4-Nanodiscs have absorption bands in the visible wavelength region, which upon binding certain drugs shift to either shorter (type I) or longer wavelengths (type II). On the basis of the coupling between the LSPR of the Ag nanoparticles and the electronic resonances of the heme chromophore in CYP3A4-Nanodiscs, LSPR spectroscopy is used to detect drug binding with high sensitivity. This paper combines LSPR and Nanodisc techniques to optically sense drug binding to a functionally stable membrane protein, with the goal of integrating this with microfluidics and expanding it into a multiarray format, enabling high-throughput screening.

In the drug development field, there is an intense search for novel label-free techniques that can be used for analysis of biomolecular interactions.[1−4] Membrane-bound proteins are of special interest to the drug discovery community as they constitute one-third of the genome and make up half of the pharmaceutically relevant drug targets.[3] In particular, human membrane-bound cytochrome P450s are key players in drug−drug interactions which can potentially lead to drug toxicity.[5,6] However as, membrane-bound P450s tend to denature and become inactive both in solution and on surfaces, there is great interest in developing techniques that can stabilize membrane proteins on surfaces and allow rapid screening of drug candidates against P450s.

Lately, several sensor concepts have emerged which are based on optical, electrical, or mechanical signal transduction. Nanoplasmonics-based optical detection methods are particularly attractive as they can be miniaturized.[3,4]

One widely used technique is optical sensing based on the excitation of propagating surface plasmon polaritons, also known as surface plasmon resonance (SPR), on metallic surfaces.[3,7] SPR is the coherent oscillation of the surface conducting electrons, which are excited when light impinges on thin metallic films. SPR is extremely sensitive to the refractive index of the surrounding medium. Sensing based on the dielectric sensitivity of SPR has been extensively used as a label-free technique to analyze various molecular recognition events involving proteins and small molecules.[8−10] However, the conventional SPR sensing scheme based on the change in bulk refractive index cannot be used reliably to detect the binding of very small molecules (<500 Da) to large analytes such as proteins.

Another optical sensing method is based on localized surface plasmon resonance (LSPR), which arises when light interacts with particles much smaller than the wavelength of the incident light. Similar to the SPR, the LSPR is highly dependent on the refractive index of the surrounding media. Upon analyte binding, the extinction maximum wavelength (λ_{max}) of the nanoparticle shifts, which has been used for chemical and biological sensing.[11−18] Moreover, since the LSPR is highly localized around the nanoparticle, it is more sensitive to the changes in the local environment near the nanoparticle surface compared to SPR. Therefore, LSPR can be used to observe the conformational changes of the adsorbed species on the nanoparticle surface.[19]

A new LSPR detection mechanism has recently been demonstrated, based on the strong coupling between the molecular resonances of chromophores and the nanoparticle LSPR.[20−23] Studies revealed that the LSPR shift from resonant analyte binding

* To whom correspondence should be addressed. E-mail: schatz@chem.northwestern.edu (G.C.S.), s-sligar@uiuc.edu (S.G.S.), vanduyne@northwestern.edu (R.P.V.D.). Phone: (847) 491-5657 (G.C.S.), (217) 244-7395 (S.G.S.), (847) 491-3516 (R.P.V.D.). Fax: (847) 491-7713 (G.C.S.), (217) 265-4073 (S.G.S.), (847) 491-7713 (R.P.V.D.).

† University of Illinois Urbana−Champaign.

‡ Current Address: Department of Chemistry, Massachusetts Institute of Technology, 77 Massachusetts Avenue, Cambridge, Massachusetts 02139.

§ Northwestern University.

(1) Heyse, S.; Stora, T.; Schmid, E.; Lakey, J. H.; Vogel, H. *Biochim. Biophys. Acta, Biomembr.* **1998**, *1376*, 319–338.
(2) Myszka, D. G.; Rich, R. L. *Pharm. Sci. Technol. Today* **2000**, *3*, 310–317.
(3) Cooper, M. A. *Nat. Rev. Drug Discovery* **2002**, *1*, 515–528.
(4) Cooper, M. A. *J. Mol. Recognit.* **2004**, *17*, 286–315.
(5) Guengerich, F. P. *Annu. Rev. Pharmacol. Toxicol.* **1999**, *39*, 1–17.
(6) Guengerich, F. P. *Chem. Res. Toxicol.* **2008**, *21*, 70–83.
(7) Willets, K. A.; Van Duyne, R. P. *Annu. Rev. Phys. Chem.* **2007**, *58*, 267–297.
(8) Lee, H. J.; Nedelkov, D.; Corn, R. M. *Anal. Chem.* **2006**, *78*, 6504–6510.
(9) Li, Y.; Lee, H. J.; Corn, R. M. *Anal. Chem.* **2007**, *79*, 1082–1088.
(10) Homola, J. *Chem. Rev.* **2008**, *108*, 462–493.

10.1021/ac802612z CCC: $40.75
Published on Web 04/13/2009

is highly dependent on the spectral overlap between the molecular resonances and the LSPR. Specifically, a 3-fold larger shift in λ_{max} occurs when the LSPR is located at a slightly longer wavelength than the molecular resonance, in comparison to when the LSPR wavelength is distant from the molecular resonance. This phenomenon was observed for several dye molecules and has been used to detect the binding of low molecular weight substrates and inhibitors to heme proteins.[21−23] This opens up the possibility of designing an LSPR-based sensor to study drug interactions with human cytochrome P450s. The sensing platform used in the present work consists of size-tunable silver nanoparticles fabricated by nanosphere lithography (NSL).[24] Briefly, the glass substrate is drop-coated with polystyrene nanospheres which serve as a deposition mask. A silver film is then evaporated on the polystyrene nanosphere monolayer. Following the metal deposition, the polystyrene nanosphere monolayer is removed by sonication which leaves behind Ag nanoparticles periodically patterned on the glass surface. NSL can be used to control the nanoparticle size, shape, and interparticle spacing. The LSPR peaks of the nanoparticles can be controlled by changing the nanosphere diameter, which controls the in-plane width of the nanoparticles, and the deposited metal film thickness, which controls the out-of-plane height. In general, an increase in nanosphere diameter and/or a decrease in metal film thickness results in a red shift in the LSPR of the fabricated nanoparticles.

One of the cornerstones in drug discovery research is the need for ultrasensitive detection of drug interactions with membrane-bound human cytochrome P450s.[25−27] Cytochrome P450 3A4 (CYP3A4) is one of the most important enzymes in drug and xenobiotic metabolism in the human body[5] and is prone to inhibition because of its broad substrate specificity and promiscuous open active site.[28] The inhibition of CYP3A4 by one drug can modify the pharmacokinetic profile of another drug leading to variations of efficacy or even toxicity in humans.[6] Hence, the discovery of drugs which bind to this protein is an important focus in early drug discovery.

On the basis of spectral changes which CYP3A4 undergoes upon drug binding, the drugs can be classified into three types: type I (blue shift in Soret away from 415 nm), type II (red shift in Soret), and those drugs which do not cause any shift in Soret.[29] On the basis of the extreme sensitivity of LSPR to molecular resonances of chromophores, LSPR spectroscopy can be used to distinguish between type I and type II drug binding to CYP3A4 immobilized on a nanoparticle surface.

The study of membrane-associated proteins in general, and CYP3A4 in particular, is challenging as they tend to aggregate in the absence of detergents or lipids. A variety of techniques have been developed to allow the analysis of membrane-associated proteins in model native-like lipid bilayer environments.[30−32] Nanodiscs have been used to solubilize and functionally stabilize CYP3A4 and other membrane proteins.[33−36] Nanodiscs are self-assembled, soluble, and stable lipid bilayers encircled by an amphipathic protein belt (Figure 1, panels A and C). The amphipathic protein belt, also called the membrane scaffold protein (MSP) controls the size of the Nanodiscs and can help in controlling the number of targets per Nanodisc. The use of Nanodiscs permits the study of membrane proteins in well-defined, uniform, and functionally stable environments. Nanodisc is an enabling technology which stabilizes the membrane proteins in solution and on the surface and allows them to be subjected to rigorous biophysical studies.

The stability of CYP3A4 in Nanodiscs has been utilized for several applications such as solid state NMR,[37] redox potentiometry,[38] and steady-state kinetics experiments.[39] Previously, Nanodiscs have been shown to be a viable platform to stabilize membrane proteins to maintain full functionality for surface based applications using SPR[40] and SAMDI[41] (self-assembled monolayer MALDI) and mechanistic studies of ligand binding.[40] In general, membrane-bound cytochrome P450s are produced in low-yield using heterelogous expression systems. Therefore, a high-throughput optical detection of drug binding to CYP3A4 and other membrane-bound P450s using small

(11) Malinsky, M. D.; Kelly, K. L.; Schatz, G. C.; Van Duyne, R. P. *J. Am. Chem. Soc.* **2001**, *123*, 1471–1482.
(12) Haes, A. J.; Hall, W. P.; Chang, L.; Klein, W. L.; Van Duyne, R. P. *Nano Lett.* **2004**, *4*, 1029–1034.
(13) Zhao, J.; Zhang, X.; Yonzon, C. R.; Haes, A. J.; Van Duyne, R. P. *Nanomedicine* **2006**, *1*, 219–228.
(14) Larsson, E. M.; Alegret, J.; Kall, M.; Sutherland, D. S. *Nano Lett.* **2007**, *7*, 1256–1263.
(15) Ruach-Nir, I.; Bendikov, T. A.; Doron-Mor, I.; Barkay, Z.; Vaskevich, A.; Rubinstein, I. *J. Am. Chem. Soc.* **2007**, *129*, 84–92.
(16) Anker, J. N.; Hall, W. P.; Lyandres, O.; Shah, N. C.; Zhao, J.; Van Duyne, R. P. *Nat. Mater.* **2008**, *7*, 442–453.
(17) Dahlin, A. B.; Tegenfeldt, J. O.; Hook, F.; Edvardsson, M.; Rodahl, M.; Glasmastar, K.; Larsson, C.; Kasemo, B.; Rindzevicius, T.; Alaverdyan, Y.; Dahlin, A.; Sutherland, D. S.; Kall, M.; Bramfeldt, H.; Wingren, C.; Borrebaeck, C.; Asberg, P.; Bjork, P.; Inganas, O.; Stengel, G.; Knoll, W.; Zach, M.; Reimhult, E.; Stadler, B.; Falconnet, D.; Pfeiffer, I.; Voros, J.; Graneli, A.; Rydstrom, J.; Svedhem, S.; Fant, C.; Elwing, H. *Anal. Chem.* **2006**, *78*, 4416–4423.
(18) Jonsson, M. P.; Jonsson, P.; Dahlin, A. B.; Hook, F. *Nano Lett.* **2007**, *7*, 3462–3468.
(19) Hall, W. P.; Anker, J. N.; Lin, Y.; Modica, J.; Mrksich, M.; Van Duyne, R. P. *J. Am. Chem. Soc.* **2008**, *130*, 5836–5837.
(20) Haes, A. J.; Zou, S.; Zhao, J.; Schatz, G. C.; Van Duyne, R. P. *J. Am. Chem. Soc.* **2006**, *128*, 10905–10914.
(21) Zhao, J.; Das, A.; Zhang, X.; Schatz, G. C.; Sligar, S. G.; Van Duyne, R. P. *J. Am. Chem. Soc.* **2006**, *128*, 11004–11005.
(22) Zhao, J.; Jensen, L.; Sung, J.; Zou, S.; Schatz, G. C.; Van Duyne, R. P. *J. Am. Chem. Soc.* **2007**, *129*, 7647–7656.
(23) Zhao, J.; Das, A.; Schatz, G. C.; Sligar, S. G.; Van Duyne, R. P. *J. Phys. Chem. C* **2008**, *112*, 13084–13088.
(24) Haynes, C. L.; Van Duyne, R. P. *J. Phys. Chem. B* **2001**, *105*, 5599–5611.
(25) Crespi, C. L.; Miller, V. P.; Penman, B. W. *Anal. Biochem.* **1997**, *248*, 188–190.
(26) White, R. E. *Annu. Rev. Pharmacol. Toxicol.* **2000**, *40*, 133–157.
(27) Zlokarnik, G.; Grootenhuis, P. D. J.; Watson, J. B. *Drug Discovery Today* **2005**, *10*, 1443–1450.
(28) Scott, E. E.; Halpert, J. R. *Trends Biochem. Sci.* **2005**, *30*, 5–7.
(29) Dawson, J.; Andersson, L.; Sono, M. *J. Biol. Chem.* **1982**, *257*, 3606–3617.
(30) Tamm, L. K.; McConnell, H. M. *Biophys. J.* **1985**, *47*, 105–113.
(31) Rigaud, J.-L.; Pitard, B.; Levy, D. *Biochim. Biophys. Acta, Bioenerg.* **1995**, *1231*, 223–246.
(32) Knoll, W.; Frank, C. W.; Heibel, C.; Naumann, R.; Offenhausser, A.; Ruhe, J.; Schmidt, E. K.; Shen, W. W.; Sinner, A. *J. Biotechnol.* **2000**, *74*, 137–158.
(33) Bayburt, T. H.; Sligar, S. G. *Protein Sci.* **2003**, *12*, 2476–2481.
(34) Baas, B. J.; Denisov, I. G.; Sligar, S. G. *Arch. Biochem. Biophys.* **2004**, *430*, 218–228.
(35) Leitz, A. J.; Bayburt, T. H.; Barnakov, A. N.; Springer, B. A.; Sligar, S. G. *Biotechniques* **2006**, *40*, 601–612.
(36) Nath, A.; Atkins, W. M.; Sligar, S. G. *Biochemistry* **2007**, *46*, 2059–2069.
(37) Kijac, A. Z.; Li, Y.; Sligar, S. G.; Rienstra, C. M. *Biochemistry* **2007**, *46*, 13696–13703.
(38) Das, A.; Grinkova, Y. V.; Sligar, S. G. *J. Am. Chem. Soc.* **2007**, *129*, 13778–13779.
(39) Denisov, I. G.; Baas, B. J.; Grinkova, Y. V.; Sligar, S. G. *J. Biol. Chem.* **2007**, *282*, 7066–7076.
(40) Shaw, A. W.; Pureza, V. S.; Sligar, S. G.; Morrissey, J. H. *J. Biol. Chem.* **2007**, *282*, 6556–6563.
(41) Marin, V. L.; Bayburt, T. H.; Sligar, S. G.; Mrksich, M. *Angew. Chem., Int. Ed. Engl.* **2007**, *46*, 8796–8798.

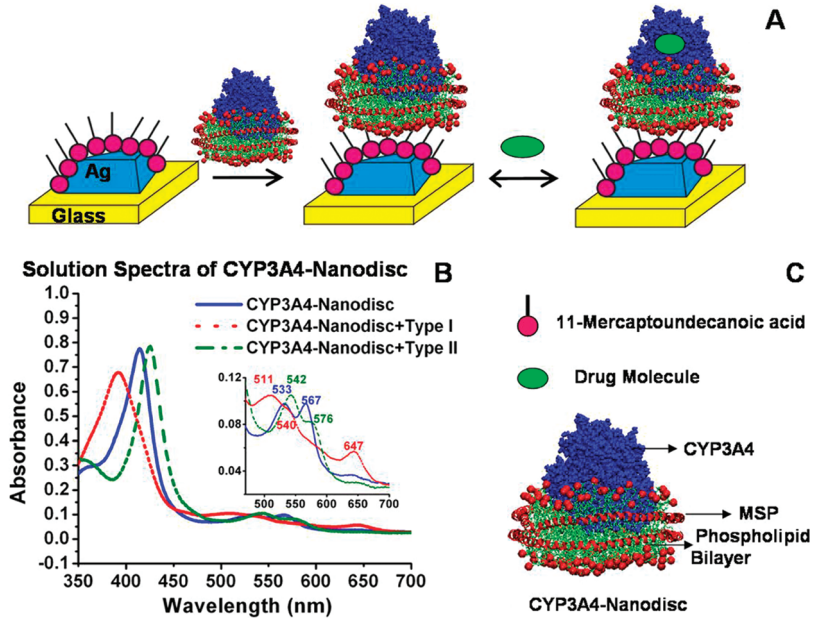

Figure 1. (A) Schematic representation of CYP3A4-Nanodisc immobilized Ag nanobiosensor fabricated using nanosphere lithography (NSL), following by the binding of a drug molecule to the protein immobilized on the surface. (B) Solution UV−Vis absorption spectra of CYP3A4-Nanodisc in the following states: (1) low spin substrate free ferric state with a Soret band at 415 nm (blue solid line), (2) high spin type I drug bound ferric state with a Soret band at 391 nm (red dotted line), and (3) low spin type II drug bound ferric state with Soret band at 425 nm (green dashed line). The inset shows the detailed changes in the Q-band region. (C) Schematic notations of 11-MUA, the drug and CYP3A4-Nanodiscs. CYP3A4 is shown as a blue space filled model inserted into Nanodiscs. Nanodiscs are nanometer sized discoidal particles with two membrane scaffold proteins (MSP) shown in red ribbon wrapped around a lipid bilayer (shown with the lipid headgroups in red, and the lipid tails in green) in a belt-like manner.

quantities of protein would be an important contribution to the initial drug discovery process.

In the work presented here, we develop a nanoparticle-based sensor prototype for detecting drug binding to membrane proteins in a supported lipid bilayer system. Different types of drugs when bound to human membrane CYP3A4 in Nanodiscs induce different shifts in the optical absorption spectra of the heme prosthetic group. Herein, we demonstrate that these binding events can be detected with high sensitivity using localized surface plasmon resonance spectroscopy.

MATERIALS AND METHODS

Materials. Silver shot was purchased from Alfa Aesar (#11357 1−3 mm diameter, Premion, 99.9999%). Tungsten vapor deposition boats were acquired from R.D. Mathis (Long Beach, CA). Polystyrene nanospheres with diameters of 280 ± 4 nm were received as a suspension in water (Interfacial Dynamics Corporation, Portland) and were used without further treatment. The buffer salts ($KH_2PO_4 \cdot 3H_2O$ and KH_2PO_4) and fisherbrand No. 2 glass coverslips with 18 mm diameter were obtained from Fisher Scientific (Pittsburgh, PA). For all steps of substrate preparation, water purified to a resistivity of 18.2 MΩ·cm with Millipore cartridges (Marlborough, MA) was used.

1-Ethyl-3-[3-dimethylaminopropyl]carbodiimide hydrochloride (EDC) was purchased from Pierce (Rockford, IL). Sodium cholate, 11-mercaptoundecanoic acid (11-MUA), bromocriptine (BC), erythromycin (ERY), testosterone (TST), lovastatin (LVS), androstenedione (ADS), alpha-naphthoflavone (ANF), nifedipine (NFD), ketoconazole (KTC), itraconazole (ITZ), tranylcypromine (TCA), diclofenac (DCF), terfenadine (TRF), and Amberlite (XAD-2) were purchased from Sigma-Aldrich-Fluka. CHAPS is from Anatrace, Inc. (Maumee, OH), Emulgen 913 from Karlan Research Products Corp. (Santa Rosa, CA); and POPC (1-Palmitoyl-2-Oleoyl-*sn*-Glycero-3-Phosphocholine) from Avanti Polar Lipids Inc. (Alabaster, AL).

Expression and Purification of CYP3A4 Nanodiscs. Cytochrome P450 3A4 (CYP3A4) with a C-terminal histidine tag was expressed from the NF-14 construct in the PCWori+ vector as previously described.[34,39,42−44] The CYP3A4 in NF-14 pCWOri+ vector was a generous gift from Dr. F. P. Guengerich (Vanderbilt University, Nashville, TN). CYP3A4 was expressed and purified from *Escherichia coli* as previously described with minor modifications.[34]

Human CYP3A4 was assembled into Nanodiscs using the membrane scaffold protein MSP1D1(-),[45] in which the poly(histidine) tag is removed.[34] Briefly, purified CYP3A4 (in 0.1% Emulgen 913) from the *E. coli* expression system was mixed with the disk reconstitution mixture containing MSP1D1(-), POPC, and sodium cholate present in 1:65:130 molar ratios. The ratio of CYP3A4/MSP1D1(-) was kept at 1:10. The detergents (cholate and Emulgen) were removed by treatment with Amberlite (XAD-2), to initiate the self-assembly of Nanodiscs. The resultant mixture was then purified using Ni-NTA column to remove the empty Nanodiscs followed by size exclusion chromatography to obtain homogeneous CYP3A4-Nanodiscs in 100 mM potassium phosphate buffer (pH 7.4).

The result of this self-assembly reaction is monomeric CYP3A4 incorporated into a 10 nm discoidal POPC bilayer stabilized by the encircling amphipathic membrane scaffold protein belt. The CYP3A4-Nanodiscs were prepared in a substrate-free form and

(42) Domanski, T. L.; Liu, J.; Harlow, G. R.; Halpert, J. R. *Arch. Biochem. Biophys.* **1998**, *350*, 223–232.
(43) Hosea, N. A.; Miller, G. P.; Guengerich, F. P. *Biochemistry* **2000**, *39*, 5929–5939.
(44) Gillam, E. M. J.; Baba, T.; Kim, B. R.; Ohmori, S.; Guengerich, F. P. *Arch. Biochem. Biophys.* **1993**, *305*, 123–131.
(45) Denisov, I. G.; Grinkova, Y. V.; Lazarides, A. A.; Sligar, S. G. *J. Am. Chem. Soc.* **2004**, *126*, 3477–3487.

kept at 4 °C. For long-term storage, the preparations were flash frozen and stored in −80 °C in the presence of 10% glycerol.[46] The CYP3A4-Nanodiscs concentration was measured by UV-vis spectroscopy with a Cary Bio 300 spectrophotometer (Varian, Lake Forest, CA) and a molar absorption coefficient $\varepsilon_{417} = 115\ mM^{-1}\ cm^{-1}$. To test the functional integrity of the protein used in the experiments, each CYP3A4-Nanodiscs preparation was evaluated for bromocriptine binding.[38]

Substrate Binding to CYP3A4 Nanodiscs in Solution. The substrate binding spectra in solution were measured using a Cary Bio 300 UV-vis spectrophotometer in dual-beam mode. CYP3A4-Nanodiscs at and optical density of 0.1 were added to the sample cuvette with a total volume of 120 μL in each. The drug molecules prepared in 10 mM to 20 mM stocks in organic solvent (ethanol, methanol, or chloroform). A small aliquot of the drug stock was added to the protein solution, keeping the concentration of the organic solvent below 1.5%. The absorption spectra were measured between 350 and 700 nm and corrected for the dilution factor.[46]

Glass Substrate Preparation. Glass substrates were cleaned in piranha solution (1:3 30% H_2O_2/H_2SO_4) for 1 h at 80 °C. Glass samples were cooled to room temperature and were then rinsed profusely with deionized (18.2 MΩ·cm) water, sonicated in 5:1:1 $H_2O/NH_4OH/30\%\ H_2O_2$ and thoroughly rinsed with deionized water. The samples were stored in deionized water prior to use.

Nanoparticle Preparation. Nanosphere lithography (NSL)[24] was used to create monodisperse, surface-confined Ag nanoparticles. Polystyrene nanospheres (~2.2 μL) were drop-coated onto the glass substrates and allowed to dry, forming a monolayer in a close-packed hexagonal formation, which served as a deposition mask. The samples were then transferred to the evaporation chamber. The pressure in the vacuum chamber was maintained below 1×10^{-5} Torr during the evaporation. A silver film was evaporated on the coated glass substrates with a Ag deposition rate of 1.0 ~1.5 Å/s. A Leybold Inficon XTM/2 quartz crystal microbalance (East Syracuse, NY) was used to measure the thickness of the Ag film deposited over the nanosphere mask. Following metal deposition, the samples were sonicated for 3−5 min in ethanol to the remove the polystyrene nanosphere mask. The LSPR peaks of the nanoparticles can be fine-tuned. The in plane width of the nanoparticles can be changed by changing the nanosphere diameter used in the deposition mask. The out-of-plane height can be controlled by changing the deposited metal film thickness. In this work, the nanoparticles were fabricated with LSPR in the 500−600 nm range for the 11-MUA-functionalized nanoparticles. To achieve this, the nanosphere used as masks were 280 nm in diameter, and the height of silver deposition was 50 nm.

Nanoparticle Solvent Annealing and Functional Immobilization. For each experiment, the Ag nanoparticles on glass substrate sample was stabilized and functionalized in a home-built flow cell. Immediately following nanosphere removal, the samples were placed in solution of 1 mM 11-MUA (in ethanol) for 24−48 h, which reproducibly yields approximately full monolayer coverage of 11-MUA. After incubation, the nanoparticle samples were rinsed thoroughly with neat ethanol and dried by flowing N_2 gas through the sample cell. Samples were then activated using 10 mM EDC mixed with 1 μM CYP3A4-Nanodiscs for 1 h. After incubation, the nanoparticle samples were rinsed with deionized water and dried by flowing N_2 gas through the sample cell. Finally, the samples were incubated in 200 μM drug compounds in buffer solution for 30 min. After incubation, the nanoparticle samples were gently rinsed with deionized water and dried by flowing N_2 gas through the sample cell.

UV−Vis Spectroscopy on Nanoparticle Surface. Macroscale UV−Vis extinction measurements on nanoparticle surface were collected using an Ocean Optics (Dunedin, FL) SD2000 fiber optically coupled spectrometer with a CCD detector and a Cary 300 Bio UV−Vis spectrophotometer. All spectra in this study are macroscopic measurements performed in standard transmission geometry with unpolarized light. The extinction spectra of the same sample acquired from the two spectrometers were calibrated.

RESULTS AND DISCUSSION

Drug Binding to CYP3A4-Nanodiscs in Solution. Drug binding to CYP3A4-Nanodiscs in solution was monitored using UV−Vis absorption spectroscopy (350−700 nm). The substrate-free CYP3A4 in Nanodiscs is low spin and has a Soret band at ~415 nm, a less intense α-Q-band at 567 nm, and a β-Q-band at 532 nm (Figure 1B). The binding of various drug molecules to CYP3A4 gives rise to two characteristic types of spectral changes which are indicative of the primary mode of small molecule binding to CYP3A4 as discussed before.[29]

Type I drugs modulate the ferric spin state of the heme by displacing a coordinated water molecule occupying the sixth coordinate site of the heme iron.[29] The binding of type I drugs induces a spectral change in the Soret band from 415 to 391 nm, as shown in Figure 1B. There is also a decrease in the intensity of the α-Q-band relative to β-Q-band. Moreover, there is a blue shift of the α-Q-band from 567 to 540 nm and of the β-Q-band from 532 to 511 nm, and the appearance of a charge transfer band at 645 nm. Type I drugs are typically substrates of CYP3A4 for enzymatic oxygenation.

Type II drugs inhibit the enzyme by binding directly to the iron, usually through a nitrogen moiety, without changing the spin state.[47] On binding nitrogen donors such as those containing imidazole, azole, or amine groups, the Soret band of CYP3A4 red shifts from 415 to 423 nm and the Q-bands shift from 567 to 576 nm and 532 to 542 nm as shown in Figure 1B. This is because the ligand field of type II drugs is stronger than that of water, and the resulting low spin complex therefore has red-shifted Soret and Q-bands compared to the substrate-free protein. In general, the strong ligand field of type II drugs results in a decrease in the redox potential of the CYP3A4 heme iron. This decrease in redox potential of CYP3A4 is associated with difficulty in reduction of the CYP3A4-drug complex by its redox partner cytochrome P450 reductase and is thought to be a general mechanism of inhibition by type II drugs.[29]

Table 1 summarizes the binding type and spectral changes produced by a variety of drugs upon binding to CYP3A4-Nanodiscs. Bromocriptine, testosterone, lovastatin, adrostenedione, alpha-naphthoflavone, erythromycin, and nifedipine show a type I shift on binding CYP3A4-Nanodiscs while ketoconazole, itraconazole, tranylcypromine, diclofenac, and terfenadine show a type II shift on binding CYP3A4-Nanodiscs.

(46) Denisov, I. G.; Grinkova, Y. V.; Baas, B. J.; Sligar, S. G. *J. Biol. Chem.* **2006**, *281*, 23313–23318.
(47) Ahlstrom, M. M.; Zamora, I. *J. Med. Chem.* **2008**, *51*, 1755–1763.

Table 1. Drug Binding to CYP3A4-Nanodiscs Immobilized on Silver Nanoparticles

	Drug	Binding type (solution)	Direction of LSPR shift (surface)	Amount of LSPR shift
1	Bromocriptine (dopamine agonist)	Type I	Blue	(−) 8 nm
2	Testosterone (steroid hormone)	Type I	Blue	(−) 7 nm
3	Lovastatin (lipid lowering)	Type I	Blue	(−) 4 nm
4	Androstene-dione (steroid hormone)	Type I	Blue	(−) 6 nm
5	Alpha-naphthoflavone (flavonoid prototype)	Type I	Blue	(−) 8 nm
6	Nifedipine (calcium channel blocker)	Type I	Blue	(−) 4 nm
7	Erythromycin (macrolide antibiotic)	Type I	Blue	(−) 1 nm
8	Ketoconazole (antifungal)	Type II	Red	(+) 4 nm
9	Itraconazole (antifungal)	Type II	Red	(+) 2 nm
10	Tranylcypromine (monoamine oxidase inhibitor)	Type II	Red	(+) 2 nm
11	Diclofenac (anti-inflammatory)	Type II	Red	(+) 5 nm
12	Terfenadine (antihistamine)	Type II	Red	(+) 3 nm

CYP3A4-Nanodiscs Binding to Silver Nanoparticles. Nanosphere lithography (NSL) was used to create monodisperse, surface-confined triangular Ag nanoparticles. To study drug binding using LSPR, there are two steps after the nanoparticles are functionalized with a self-assembled monolayer (SAM) of 11-MUA (Schematic illustrated in Figure 1A). First, with the aid of EDC, CYP3A4-Nanodiscs are covalently bound to the carboxyl terminated groups on 11-MUA. The second step is the binding of drug molecules to the surface-bound CYP3A4-Nanodiscs. The LSPR of the sample during each experimental step is monitored using UV−Vis extinction spectroscopy in a N_2 environment as shown if Figure 2D-F.

The coupling of the CYP3A4-Nanodiscs to the LSPR is wavelength-dependent; when the LSPR of the MUA-functionalized nanoparticles is 500−600 nm, the average LSPR shift upon CYP3A4-Nanodiscs addition is 35−40 nm ($\lambda_{max,CYP3A4\text{-}ND} - \lambda_{max,MUA}$), as shown in Figure 2D−F. This wavelength range was chosen for convenience in the fabrication of the NSL particles, and does not overlap with the strong Soret excitation of the protein, where larger shifts are likely.

The surface area of the nanoparticle is 1.4×10^{-10} cm^2 and the jamming limit fraction of Nanodiscs on the surface is 0.547.[48] The area of a Nanodisc lying flat on the surface is 7.9×10^{-13} cm^2; therefore, the total number of Nanodiscs on a single nanoparticle is ∼100, assuming the Nanodics are closely packed. The probe spot in these experiments is $\sim 7.8 \times 10^{-3}$ cm^2 (1 mm diameter), and the density of the nanoparticles is 1.5×10^9 nanoparticles/cm^2; hence, there are 1.2×10^7 nanoparticles in the probing area. Therefore, the readable output in this case is from 1.2×10^9 Nanodiscs, which corresponds to femtomoles of Nanodiscs. With single nanoparticle spectroscopy,[49] this number can be reduced to ∼100 Nanodiscs. From these calculations, it can be inferred that this system is highly sensitive and can generate readable optical output from a very few protein molecules on the surface. This technique can also be applied

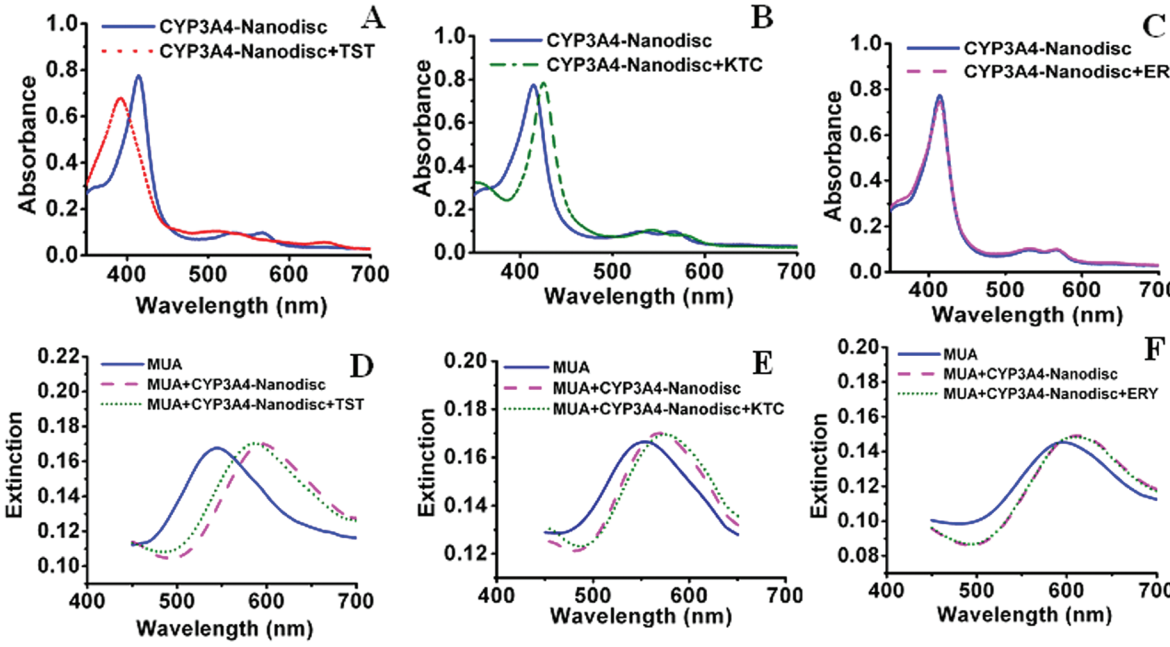

Figure 2. (Top panel): (A) (B) (C) Solution UV−Vis absorption spectrum of CYP3A4-Nanodisc with testosterone (TST) bound (type I substrate), Ketoconazole (KTC) bound (Type II drug), and Erythromycin (ERY) bound (shows a very small type I shift). (Bottom panel): Surface UV−Vis extinction spectra of each step in the surface modification of NSL fabricated Ag nanoparticles for the different drug molecules. (D) Testosterone (representative type I substrate) binding, $\lambda_{max,MUA} = 547$ nm, $\lambda_{max,CYP3A4\text{-}ND} = 596$ nm, and $\lambda_{max,CYP3A4\text{-}ND\text{-}Type\ I} = 589$ nm (blue shift). (E) Ketoconazole (representative type II substrate), $\lambda_{max,MUA} = 553$ nm, $\lambda_{max,CYP3A4\text{-}ND} = 566$ nm, and $\lambda_{max,CYP3A4\text{-}ND\text{-}KTC} = 570$ (red shift). (F) Erythromycin binding, $\lambda_{max,MUA} = 591$ nm, $\lambda_{max,CYP3A4\text{-}ND} = 610$ nm and $\lambda_{max,CYP3A4\text{-}ND\text{-}ERY} = 609$ nm. All extinction measurements were collected in a N_2 environment.

to any other protein containing a chromophore and is hence useful in the study of drug binding to proteins which are available in very low quantity.

Drug Binding to CYP3A4-Nanodiscs on Nanoparticle Surface as Monitored Using LSPR. Figure 2shows three sets of representative spectra for the drug molecules which were tested for binding to CYP3A4-Nanodiscs. The top panels (Figure 2A−C) show the shift in the solution spectrum on binding of the drug molecules to the protein. The bottom panels (Figure 2D−F) show the UV−Vis extinction spectra of each step in the surface modification of NSL fabricated Ag nanoparticles for the different drug molecules. For instance, in Figure 2D, the thiol modified nanoparticle has $\lambda_{max,MUA} = 547$ nm. On immobilization of CYP3A4 Nanodiscs, $\lambda_{max,CYP3A4\text{-}ND}$ is 596 nm. On binding testosterone (TST), a representative type I substrate, the $\lambda_{max,CYP3A4\text{-}ND\text{-}TST}$ is then blue-shifted to 589 nm. The change in the LSPR maxima on binding testosterone is (−) 7 nm. The direction of shift is the same as the direction in which the Soret and the Q-bands shift on binding the testosterone drug molecules in solution (Figure 2A). As shown in Table 1, type I drugs shift the LSPR maxima to blue wavelength on binding to CYP3A4-ND immobilized on the surface of the nanoparticle, which is consistent with the changes that these drugs induce in the solution spectra.

In Figure 2E, ketoconazole (KTC), a representative type II drug, is detected with the LSPR of the nanoparticle. The thiol modified nanoparticle has $\lambda_{max,MUA} = 553$ nm. On binding CYP3A4-ND the $\lambda_{max,CYP3A4\text{-}ND} = 566$ nm, and on binding ketoconazole, $\lambda_{max,CYP3A4\text{-}ND\text{-}KTC}$ is further red-shifted to 570 nm. The change in the LSPR maxima of the nanoparticle on binding ketoconazole is (+) 4 nm. The direction of shift is in the same as the direction in which the Soret and the Q-bands shift on binding the ketoconazole drug molecules in Figure 2B. Other type II drugs also produce a red shift when they bind to CYP3A4-Nanodiscs on the nanoparticle surface (Table 1). The LSPR shift in λ_{max} on binding a type II drug is less than those observed for type I drug molecules. This is because, the LSPR shifts observed are a manifestation of the coupling between the nanoparticle and the protein chromophore, and if the protein solution spectrum shows less changes due to substrate/inhibitor binding then the LSPR peaks will also change to a lesser extent.[23]

Another interesting case is that of erythromycin (ERY), which on binding to the protein produces minimal changes in the protein spectra as shown in Figure 2C. On binding erythromycin to CYP3A4-ND on nanoparticle surface, the LSPR maxima are the following: $\lambda_{max,MUA} = 591$ nm, $\lambda_{max,CYP3A4\text{-}ND} = 610$ nm, and $\lambda_{max,CYP3A4\text{-}ND\text{-}ERY} = 609$ nm. The LSPR peak is blue-shifted by (−) 1 nm. This shows that there is a correlation between the amount of shift produced in spectral bands on drug binding to the protein in solution and the LSPR shifts produced on drug binding to the protein on the surface of the nanoparticle. This observation is consistent with the previous observations from substrate or inhibitor binding to P450cam[23]

Table 1 and Figure 2 demonstrate that it is possible to detect and distinguish between the binding of type I and type II drugs to CYP3A4-Nanodiscs using LSPR. The direction of the LSPR shift is consistent with the shifts observed in the protein solution spectra on binding type I and II drugs. At the LSPR wavelengths used in these studies, for type I drugs the blue shift is ∼6−8 nm and for type II drugs the red shift is ∼1−4 nm. These shifts are smaller than were obtained in our previous work with a non-membrane-bound P450 protein (CYP101), as might be expected given that the protein coverage with the Nanodiscs is expected to be lower.[23] In addition, the present measurements did not involve nanoparticles whose size generates maximal overlap of the LSPR and molecular resonances. Nevertheless, the observation of these drug-induced LSPR shifts is still quite feasible.

For obtaining spectral changes due to drug binding to CYP3A4-Nanodiscs, it is extremely important for the protein to be in the active and in a native state on the surface. Often membrane proteins denature or unfold on the surfaces. Here, Nanodiscs maintain an active P450 with no evidence of P420 formation while on the silver nanoparticle.

CONCLUSION

In this paper, we report one of the few known membrane protein biosensors which detects the binding of small drug molecules (M.W. ∼100−700 Da), in this case to membrane-bound cytochrome CYP3A4-Nanodisc. Using the technique, we can successfully distinguish two types of drug binding to CYP3A4-Nanodisc. These binding events induce a change in the electronic structure of the protein but do not lead to any significant changes in the bulk refractive index of the surrounding medium. Therefore, small molecule binding is hard to detect by conventional SPR based methods that are only sensitive to bulk refractive index change. The resonant coupling method described herein is more sensitive than solution UV−Vis spectroscopy of proteins. This work opens up new avenues to detect ligand-membrane protein interactions using LSPR. Furthermore, the combination of the Nanodisc technology with LSPR makes it possible to rapidly screen for binding of multiple drug candidates to membrane proteins. The fact that the LSPR detection modality can be integrated with microfluidics[50] and expanded into a multiarray format makes it a promising methodology for large-scale drug screening to membrane-bound cytochrome P450s.

ACKNOWLEDGMENT

We acknowledge Dr. Ilia Denisov at University of Illinois Urbana−Champaign for helpful comments. This research was supported by the National Science Foundation (EEC-0647560, CHE-0414554, DMR-0520513, BES-0507036), the DTRA JSTO Program (FA9550-06-1-0558), AFOSR/DARPA Project BAA07-61 (FA9550-08-1-0221), and the National Cancer Institute (1 U54 CA119341-01). Any opinions, findings and conclusions or recommendations expressed in this material are those of the authors and do not necessary reflect those of the National Science Foundation.

(48) Feder, J. *J. Theor. Biol.* **1980**, *87*, 237–254.
(49) McFarland, A. D.; VanDuyne, R. P. *Nano Lett.* **2003**, *3*, 1057–1062.
(50) Goluch, E. D.; Shaw, A. W.; Sligar, S. G.; Liu, C. *Lab Chip* **2008**, *8*, 1723–1728.

Received for review December 11, 2008. Accepted March 25, 2009.

AC802612Z